Electronic Supplementary Material (ESI) for Journal of Materials Chemistry C.
This journal is © The Royal Society of Chemistry 2022

Supplemental Materials for

Overall direct photocatalytic water-splitting on C2mm-graphyne: A novel two-dimensional carbon allotrope

Dong-Chun Yang,[a,b] **Roberts I. Eglitis,**[c] **Zhi-Jun Yi,**[d] * **Chun-Sheng Liu,**[e] **Ran Jia,**[a,c] *

[a] *Institute of Theoretical Chemistry, College of Chemistry, Jilin University, 130023 Changchun, PR China.*

[b] *Institute of Chemistry Chinese Academy of Sciences, 100190 Beijing, PR China.*

[c] *Institute of Solid State Physics, University of Latvia, 8 Kengaraga Str., Riga LV1067, Latvia.*

[d] *School of Materials and Physics, China University of Mining and Technology, 221116 Xuzhou, PR China.*

[e] *College of Electronic Science and Engineering, Nanjing University of Posts and Telecommunications, 210046 Nanjing, PR China.*

* *Correspondence to*:
zhijunyi@cumt.edu.cn (Zhi-Jun Yi)
jiaran@jlu.edu.cn (Ran Jia)

1 Atomic configuration of C2mm-graphyne

$POSCAR - CGY$		
1.00000000000000		
7.3773999214	0.0000000000	0.0000000000
0.0000157993	9.1269998550	0.0000000000
0.0000000000	0.0000000000	25.0000000000
C		
32		
$Direct$		
0.176630005	0.859839976	0.472209990
0.746680021	0.240170002	0.556710005
0.823409975	0.128839999	0.427899987
0.676630020	0.359840006	0.472209990
0.246680006	0.740170002	0.556710005
0.323410004	0.628840029	0.427899987
0.176630005	0.129859999	0.527790010
0.746680021	0.749530017	0.443289995
0.823409975	0.860859990	0.572109997
0.676630020	0.629859984	0.527790010
0.246680006	0.249530002	0.443289995
0.323410004	0.360859990	0.572109997
0.176630005	0.129859999	0.472209990
0.746680021	0.749530017	0.556710005
0.823419988	0.860859990	0.427890003
0.676630020	0.629859984	0.472209990
0.246680006	0.249530002	0.556710005
0.323419988	0.360859990	0.427890003
0.176630005	0.859839976	0.527790010
0.746680021	0.240170002	0.443289995
0.823409975	0.128839999	0.572099984
0.676630020	0.359840006	0.527790010
0.246680006	0.740170002	0.443289995
0.323410004	0.628840029	0.572099984
0.922370017	0.994849980	0.571870029
0.096620001	0.994849980	0.551419973
0.422369987	0.494850010	0.571870029
0.596620023	0.494850010	0.551419973
0.922370017	0.994849980	0.428130001
0.096620001	0.994849980	0.448579997
0.422369987	0.494850010	0.428130001
0.596620023	0.494850010	0.448579997

Table S1 The lattice parameters, cohesive energies, and band gaps of the pristine C2mm-graphyne and its doped systems.

Systems	lattice parameter (Å)		E_{coh} (eV/atom)	Band gap (eV)	
	a	b		PBE	GW
pristine	9.127	7.377	-7.06	1.05	3.06
B1N5	9.318	7.292	-6.51	0.19	1.82
B5N1	9.174	7.375	-6.52	0.56	2.42
B1N5-B5N1	9.253	7.333	-6.53	1.71	3.83
B2	9.332	7.546	-6.88	0.46	1.37
B3	9.490	7.611	-6.74		metallic
B4	9.261	6.983	-6.95	0.59	1.76
N1	8.943	7.375	-6.45		metallic
N5	9.127	7.377	-6.44		metallic
g-C_3N_4	4.780	4.780	-6.02	1.574	3.123 (HSE06)[1]

2 Doped systems

2.1 Geometric configurations

There are eight different doping configurations considered in this study, as shown in Fig. S1. Note that only B2, B4, and B5N1 systems are structurally stable semiconductors. Therefore, these three systems are focused in the present work. Of course, there exist also many other doping configurations with B or N atoms, and BN pairs. Here, we only try to propose certain doped systems to excavate the application potential of our designed C2mm-graphyne.

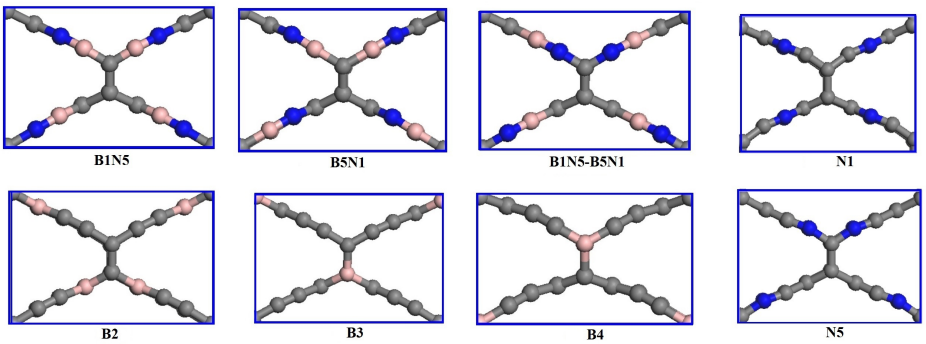

Figure S1 The sketches for the doped C2mm-graphyne systems by B-N pair or single B/N atom. The pink and blue spheres represent the B and N atoms, respectively.

2.2 Mechanical properties

For a stable 2D material, the elastic constants should satisfy Born-Huang criteria: $C_{11}C_{22}-C_{12}^2 > 0$ and $C_{66} > 0$. As shown in Table. S1, the B1N5 system is instable due to the violation of the first criterion $C_{11}C_{22} - C_{12}^2 < 0$. The Young's modulus is one of the important criteria to evaluate the mechanical strength. For 2D materials, the

Young's moduli in the Cartesian [10] and [01] directions can be described by:

$$Y_{[10]} = \frac{C_{11}C_{22} - C_{12}^2}{C_{22}}, \quad (1)$$

$$Y_{[01]} = \frac{C_{11}C_{22} - C_{12}^2}{C_{11}}. \quad (2)$$

As exhibited in Table. S1, the mechanical properties of these systems are all anisotropic. For instance, the Young's moduli in the Cartesian [10] direction are all much stronger than them in the [01] direction. Note that in the [10] direction, these systems are stronger than α-graphyne. Especially for the B2 system, the corresponding value can bear comparison with the β-graphyne. But, these material systems are relatively weak in their [01] directions.

Table S2 The calculated Young's moduli in the Cartesian [10] and [01] directions for pristine C2mm-graphyne and its doped systems. For comparison, the in-plane Young's moduli of some other 2D materials have also been calculated. Note that all the results are reported in units of N/m.

Systems	C_{11}	C_{12}	C_{22}	C_{66}	$Y_{[10]}$	$Y_{[01]}$
Pristine	134.40	46.42	26.29	43.42	52.45	10.26
B1N5	-217.53	95.72	-34.31	13.25	49.52	7.81
B5N1	95.09	30.94	17.28	32.27	40.58	7.38
B2	125.78	31.91	22.99	30.56	72.57	13.77
B4	118.02	44.40	22.40	24.73	40.05	7.32
α-graphyne	93.33	82.53	93.33	6.34	20.23	20.23
β-graphyne	129.44	88.34	129.44	19.72	68.94	68.94

2.3 Band structures

The band structures of the doped CGY systems with B, N, and B-N are exhibited in Figs. S2-S4. The Fermi levels in all of the band maps are shifted to zero. Note that the N-doped systems obviously are metallic. The B3 doped system is a p-type semiconductor. The B2 doped system possesses an indirect band gap between X and Y points. Although the B1N5-B5N1 system has a direct band gap, the gap of 3.83 eV estimated from the one-shoot G_0W_0 is too large to photocatalytic reactions.

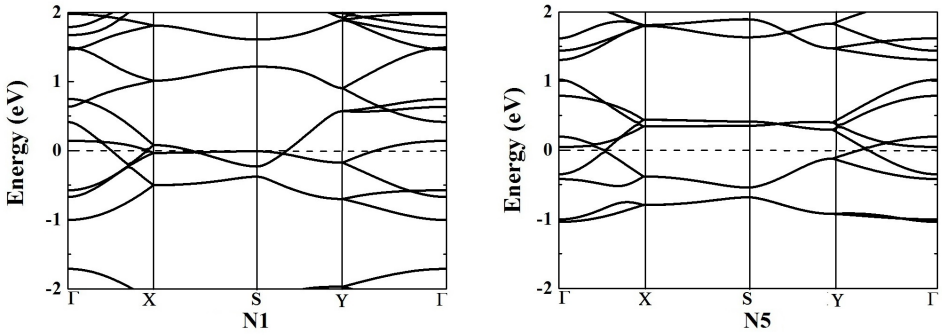

Figure S2 The band structures of the N-doped systems with PBE functional calculations at PBE level.

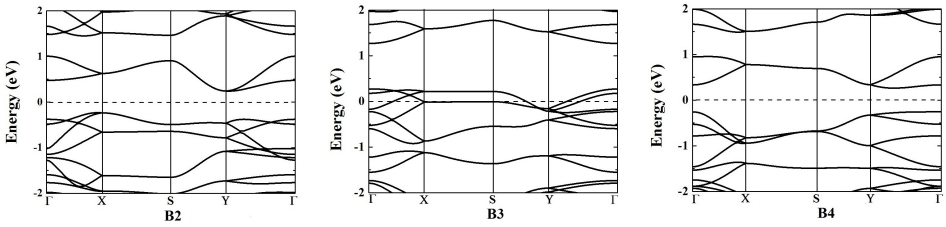

Figure S3 The band structures of the B-doped systems with PBE functional calculations at PBE level.

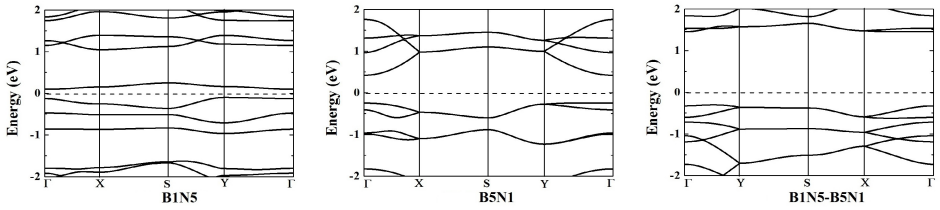

Figure S4 The band structures of the BN co-doped systems with PBE functional calculations at PBE level. Note that the B1N5 system has been determined to be instable.

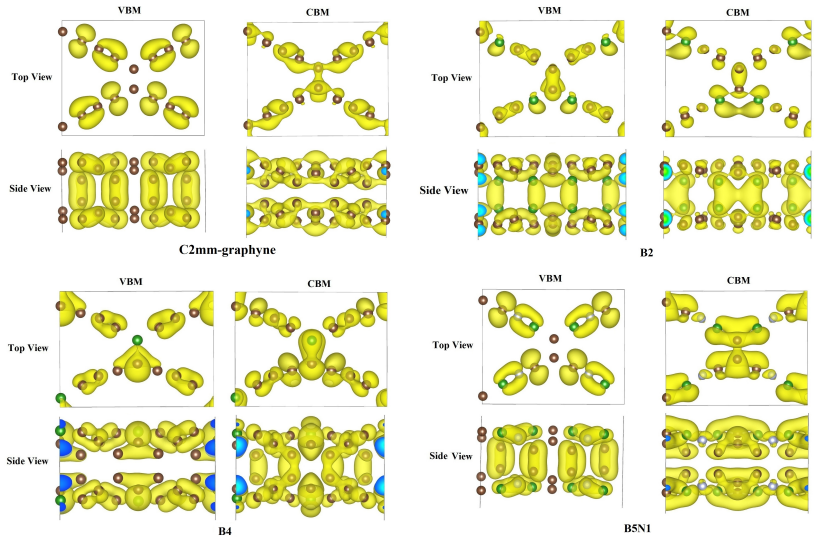

Figure S5 The top and side view of band-decomposed charge density of VBM and CBM of pristine C2mm-graphyne and its doped systems.

2.4 Stabilities

The structural stabilities of the three related doping systems B2, B4, and B5N1 are also confirmed by evaluating their phonon dispersion relations and AIMD trajectories as illustrated in Fig. S6. Obviously, there is no soft mode appearing in their phonon maps, which indicates their lattice dynamic stabilities. The root mean square deviation (RMSD) analyses of their atomic trajectories during the AIMD simulations at 1000 K confirm the thermodynamic stabilities due to relatively small atomic displacements at this relatively high temperature.

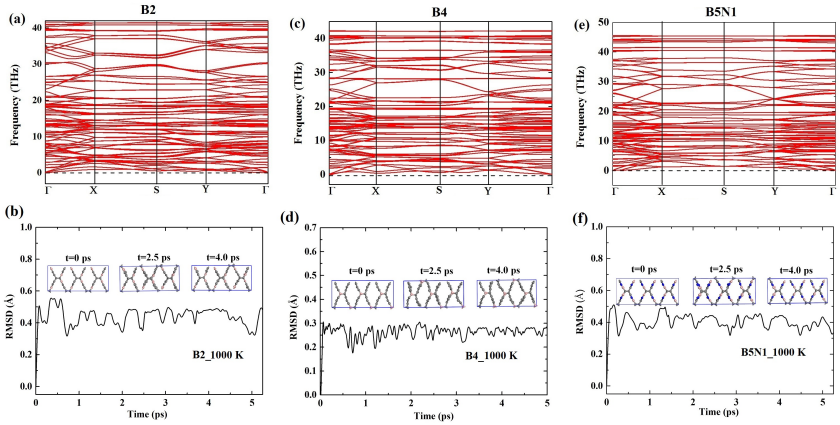

Figure S6 The phonon band maps and the RMSD curves of the doped CGY systems along the trajectories with their initial structure (at 0 ps): (a)-(b) B2 system, (c)-(d) B4 system, and (e)-(f) B5N1 system.

3 Effective mass

The inverse of effective mass $\frac{1}{m*}$ can be expressed as follows:

$$\frac{1}{m^*} = \frac{1}{\hbar^2}\frac{\partial^2 E}{\partial k^2}, \tag{3}$$

where $\hbar$ is the reduced Planck constant, E is the energy of the charge carrier, and $\vec{k}$ is the wave vector in the Brillouin zone. The energy momentum dispersion holds a parabolic relation at the valence band maximum (VBM) and the conduction band minimum (CBM). To numerically calculate the second order derivative of energy, 100 consecutive points around VBM and CBM within ± 0.01 Å^{-1} were fitted to a quadratic function.

4 Adsorption energy

To obtain the most stable adsorption configuration, all the possible adsorption sites are tested at the start. While the most preferable adsorption site can be decided by the adsorption energies:

$$E_{ad} = E_{H_2O@B4} - E_{H_2O} - E_{B4}, \tag{4}$$

where $E_{H_2O@B4}$, E_{H_2O} and E_{B4} represent the total energies of B4 doped CGY binding with H_2O molecule, the isolated H_2O molecule and the pristine B4 system.

5 Photocatalytic mechanism in water splitting

Hydrogen evolution reaction (HER) involves following reaction mechanism:

$* + H^+ + e^- \longrightarrow H^*$,

$H^* + H^+ + e^- \longrightarrow H_2 + *$.

The mechanism of oxidation reaction (OER) involves four steps:

$H_2O + * \longrightarrow HO^* + H^+ + e^-$,

$OH^* \longrightarrow O^* + H^+ + e^-$,

$O^* + H_2O \longrightarrow OOH^* + H^+ + e^-$,

$OOH^* \longrightarrow O_2 + * + H^+ + e^-$.

Therefore, the only intermediate in the reduction reaction is H^*, while the three intermediates in OER are OH^*, O^*, and OOH^*. The corresponding structures are shown in Fig. S7.

The Gibbs free energy of the adsorption of atomic hydrogen (ΔG_H) was calculated by using:

$$\Delta G_H = \Delta E_{H^*} + \Delta E_{ZPE} - T\Delta S_H,$$

where the ΔE_{H^*} is the adsorption energy of hydrogen. ΔE_{ZPE} is the change in zero-point energy, which can be calculated as follows:

$$\Delta E_{ZPE} = E^{H^*}_{ZPE} - E^{*}_{ZPE} - \frac{1}{2}E^{H_2}_{ZPE},$$

where $E^{H^*}_{ZPE}$, E^{*}_{ZPE}, and $E^{H_2}_{ZPE}$ are the zero-point energies of the clean substrate, adsorbed hydrogen, and hydrogen molecule in the gas phase, respectively. The temperature T is set to be 298.15 K, while the ΔS_H is the change in entropy of the gas phase and adsorbed hydrogen atom. These values are derived from the NIST database[4].

For the OER reactions, the free energy (ΔG_n) for each step was computed using[2, 3]:

$$\begin{aligned}
Step1 \quad &: \quad \Delta G_1 = \Delta E_1 + \frac{1}{2}E_{H_2} - E_{H_2O} + (\Delta E_{ZPE} - T\Delta S)_1 - \Delta G_U - \Delta G_{PH},\\
Step2 \quad &: \quad \Delta G_2 = \Delta E_2 + \frac{1}{2}E_{H_2} + (\Delta E_{ZPE} - T\Delta S)_2 - \Delta G_U - \Delta G_{PH},\\
Step3 \quad &: \quad \Delta G_3 = \Delta E_3 + \frac{1}{2}E_{H_2} - E_{H_2O} + (\Delta E_{ZPE} - T\Delta S)_3 - \Delta G_U - \Delta G_{PH},\\
Step4 \quad &: \quad \Delta G_4 = 4.92eV + \Delta E_4 - \frac{3}{2}E_{H_2} + 2E_{H_2O} + (\Delta E_{ZPE} - T\Delta S)_4 - \Delta G_U - \Delta G_{PH}.
\end{aligned}$$

The energy difference ΔE_n between the different surface states of the different steps can be obtained as follows:

$$\begin{aligned}
\Delta E_1 &= E_{OH^*} - E*,\\
\Delta E_2 &= E_{O^*} - E_{OH^*},\\
\Delta E_3 &= E_{HOO^*} - E_{O^*},\\
\Delta E_4 &= E* - E_{HOO^*}.
\end{aligned}$$

Note that all the results are calculated at the same conditions of pH=0 and $U = 0$ eV. The constant $(\Delta E_{ZPE} - T\Delta S)_n$ for each step can be obtained from Table S3.

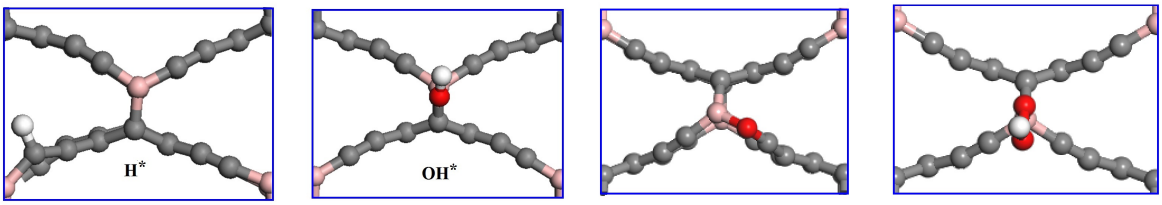

Figure S7 Optimized geometries of the related intermediates H*, OH*, O*, and OOH*.

Table S3 The calculated E and E_{ZPE} and S. The corresponding values for H_2O and H_2 can be derived from the NIST database[4].

	E (eV)	E_{ZPE} (eV)	S (eV/K)
E_*	-261.35	4.53	0.0030
E_{H*}	-264.97	4.80	0.0030
E_{*OH}	-271.89	4.88	0.0033
E_{*O}	-268.43	4.66	0.0032
E_{*OOH}	-276.45	4.89	0.0040
H_2	-6.76	0.36	0.0014
H_2O	-14.22	0.67	0.0022

References

[1] A. Mahmood, G. Shi, X. Wang, X. F. Xie, J. Sun. Photocatalytic properties of novel two-dimensional B_4C_3/g-C_3N_4 van der Waals heterojunction with moderate bandgap and high carrier mobility: A theoretical study. *Appl. Catal. B* **278**, 119310 (2020).

[2] Á.Valdés, Z. W. Qu, G. J. Kroes. Oxidation and Photo-Oxidation of Water on TiO_2 Surface. *J. Phys. Chem. C* **112**, 9872-9879 (2008).

[3] A. S. Malik, T. F. Liu, M. Dupuis, R. G. Li, C. Li. Water Oxidation on TiO_2: A Comparative DFT Study of $1e^-$, $2e^-$, and $4e^-$ Processes on Rutile, Anatase, and Brookite. *J. Phys. Chem. C* **124**, 8094-8100 (2020).

[4] M.W. Chase Jr, NIST-JANAF Themochemical Tables. *J. Phys. Chem. Ref. Data, Monograph* **9**, 1-1951 (1998).